

Coded Masks - a simulation of an astronomical γ -ray detector

Christian Schmid
supervised by J. Wilms
(Dated: July 3, 2007)

In Astronomy one cannot use conventional observation methods for high-energetic γ -rays, because they cannot be focussed by lenses or mirrors. Coded mask telescopes are one possible alternative. They are based on the observation of the shadow of the γ -rays caused by a mask with a particular pattern in the optical path. The shadow is shifted relative to the mask according to the angle of incidence. Mathematical methods like the correlation make it possible to reconstruct the position of the source, even for weak intensities and high background radiation.

Contents

I. Introduction	1
II. Theoretical background	2
A. Telescope structure	2
B. Mask layout	2
C. Coded mask telescopes	2
D. MIRAX	2
E. Mathematical methods	3
III. Program	4
A. Mask creators	4
1. Random masks	4
2. MURAs	4
B. "sample"	5
C. "analyse"	7
D. Plotting	7
IV. Simulation data	8
A. Power as a function of θ	8
B. Skyplots	8
C. Angular resolution	9
D. Intensity	9
E. Weak sources	10
V. Conclusion	11
References	11

I. INTRODUCTION

X-rays and γ -rays are high-energetic electromagnetic waves, which penetrate most materials with almost no interaction. This property makes especially the x-rays very important for medicine.

γ -rays are produced e.g. by nuclear decays and play an important role in astronomy for observing high-energetic phenomena like black holes or supernovae.

Since the atmosphere of the earth is a natural shield against γ -rays, the telescopes and other instruments have to be installed on rockets or satellites to operate in the outer space (cf. [HG], introduction p. xiv f.).

For γ -rays cannot be focussed by lenses or mirrors like optical light, one has to use alternatives like Wolter telescopes (cf. [W] or [SH]: "Wolter"). This technology has been used e.g. on the satellite "Chandra". It is based on the total reflection of γ -ray photons with a very small angle of incidence on a metal surface. Using a combination of several parabolic, hyperbolic or elliptic mirrors the γ -rays can be focussed on a detector.

However this method is only applicable up to photon energies of about 10 keV. At higher energies, as we usually have for γ -rays, we have to consider other ways of imaging, like coded masks.

In these telescopes the incident radiation is falling on a mask with a particular pattern, which is transparent at some pixels and opaque to photons at the rest of the surface. So only a part of the radiation can pass the mask and get to the underneath detector, where it creates a shadow pattern, which is determined by the coding of the mask. If the incidence angle of the radiation according to the optical axis changes, the shadow pattern is shifted. In this way, one can calculate the direction of the source of radiation from the position of the shadow on the detector relative to the mask.

A simple example is the pinhole camera: there we have a mask with one single transparent hole. The shadow and the light spot respectively on the plane behind the hole gives us the incident angle of the light, i.e. the direction of the source.

This single hole has the advantage of a positioning with high accuracy, if the hole is very narrow. But otherwise a narrow hole means little intensity of the transmitted radiation, i.e. a weak spot. This can be avoided by using several holes, which are distributed on the mask area forming a particular pattern. Of course, the shadow pattern resembles the mask pattern apart from a shift, which is caused by the position of the source according to the optical axis. So similarly to the pinhole camera the direction of the incident radiation can be determined from the shift of the shadow pattern.

When there is an overlap of shadows created by different sources of radiation, we have to use mathematical methods to reproduce the direction and intensity of each source.

In this project report you will first get some general information about coded mask telescopes and the math-

emational background (section II). Section III describes the implementation of a simulation for coded mask telescopes, the analysis program, which processes the simulation data, and some other tools. The results of several simulations are presented in section IV, focusing on the HEXIS instrument currently being designed by UC San Diego. Section V contains a summary of this project.

II. THEORETICAL BACKGROUND

A. Telescope structure

Coded mask telescopes usually consist of a γ -ray detector, the mask and a housing, which should screen off background photons coming through the sidewalls. (As the telescope is operating on a satellite and therefore has to be as lightweight as possible, the screening of the sidewalls and also the mask are usually not very perfect, so that we cannot neglect background effects.)

You can see the principle of a coded mask telescope assembly in figure 1.

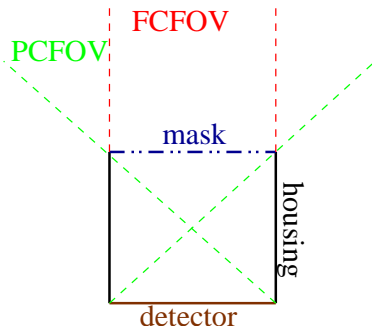


FIG. 1: basic assembly of a coded mask telescope

The mask and the detector each consist of a particular number of pixels. In general these numbers are not equal and the mask usually has a bigger area than the detector, to have a large FCFOV ("fully coded field of view", cf. [HG], p. 10). So for sources which have only a little deviation from the optical axis (i.e. lie within the FCFOV), there is no shadow from the walls on the detector.

For sources in the PCFOV ("partially coded field of view") there is always a shadow from the walls on the detector area.

This project deals with a detector and a mask of the same square size and with the same number of pixels. So the FCFOV is limited to the optical axis. All other sources that can be seen, must be at least within the PCFOV ("partially coded field of view").

B. Mask layout

The mask has a square area and consists of several pixels, which are either transparent or impenetrable for

γ -rays. (Of course a real mask cannot perfectly screen off all radiation, but this simplification is used in our model.)

The pattern should be designed in such a way, that one can achieve as good reconstruction properties as possible. As we will see later (section II E) it is important, that the correlation of the mask function has a very sharp peak at zero and very small values otherwise.

One possible approach is a mask with randomly distributed pixels and an entire opacity of about 2/3. Some simulations were performed with such a 64×64 mask, and the results turned out to be quite acceptable.

From the mathematical point of view there are better mask layouts, which are actually in use on satellites.

C. Coded mask telescopes

A popular example for a coded mask telescope actually operating on a satellite is the IBIS instrument on INTEGRAL (INTErnational Gamma-Ray Astrophysics Laboratory), which was launched on 17th of October in 2002 (cf. [UI]) and can detect γ -rays in an energy range from 15keV up to 10MeV with an angular resolution of 12arcmin. Its detector consists of two layers (CdTe and CsI) for different energy ranges with areas of 2600cm² and 3100cm² respectively (cf. [FI]).

In this project some measurement data from INTEGRAL was used to test the simulation on proper environment variables (see section IV E).

Opposite to Wolter telescopes the coded mask technology allows us to locate high energetic γ -ray sources. It also has the advantage of a quite large field of view, so one can observe whole areas of the sky at the same time without moving the telescope.

D. MIRAX

The MIRAX (Monitor e Imageador de RAios-X) mission, on which this project is based, is intended to observe γ -ray phenomena in the galactic center (see [M]) in an energy range from 10keV to 200keV.

With its large FCFOV of $7.7^\circ \times 7.7^\circ$ ([M], p. 12) it is designed for permanent observation of the galactic center and the detection of short time events.

The mask pixels of MIRAX have a width of $865\mu\text{m}$ ([M], p.16), so in this project the width of both mask and detector pixels is set to $865\mu\text{m}$. (I have used the simplification that all pixels have the same size.) The distance between mask and detector is 76cm.

The MIRAX telescope is planned to be built with a MURA ("modified uniformly redundant array") mask pattern, which is created by using prime numbers. (You can find more about the theory of mask patterns in [HG], p. 21 ff.) Most of the data in this project was created with a 151×151 MURA mask, which is intended to be used for MIRAX balloon experiments.

You can find more detailed information about MIRAX in the document [M] itself.

E. Mathematical methods

The mathematically most interesting part of this project is the analysis of the detector data, which allows us to reconstruct the directions and the intensities of several sources.

In order to do this, we define the following two functions:

- $D(x, y)$ contains the detector data: it gives the number of detector events at each detector pixel (position (x, y)). If we neglect background radiation, $D(x, y)$ is the result of the photons coming from the source and passing the mask through a transparent pixel.
- $M(x, y)$ represents the mask:

$$M(x, y) = \begin{cases} C_1 & \text{for a transparent mask pixel} \\ C_2 & \text{for an opaque pixel} \end{cases} \quad (1)$$

The constants are chosen like this:

$$C_1 = \frac{N}{N_t}$$

$$C_2 = -\frac{N}{N - N_t}$$

where N is the total number and N_t the number of transparent mask pixels.

This choice ensures that

$$\sum_{\vec{x}} M(\vec{x}) = N_t \cdot C_1 + (N - N_t) \cdot C_2 = 0 \quad (2)$$

(I use the notation $\vec{x} = \begin{pmatrix} x \\ y \end{pmatrix}$. Although the following plots usually show the one-dimensional case for convenience, one can easily generalise the ideas to two dimensions.)

Since we have a finite number of detector elements, the detector data can only be resolved up to some discrete values for \vec{x} . For convenience we choose the same grid size for the detector and for the mask.

For the simple one-dimensional mask with 8 pixels in figure 2 the function $M(x)$ and $D(x)$ may look like in figure 3.

From these data we can reconstruct the position of the source on the sky-projection plane $S(\vec{x})$ using simple trigonometric methods, as you can see in figure 4.

In our example the form of the detector data is shifted relative to the mask by exactly 1 pixel to the right.

$$\theta = \arctan\left(\frac{b}{8h}\right) \quad (3)$$

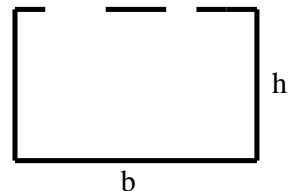


FIG. 2: example of a simple 1-dimensional mask

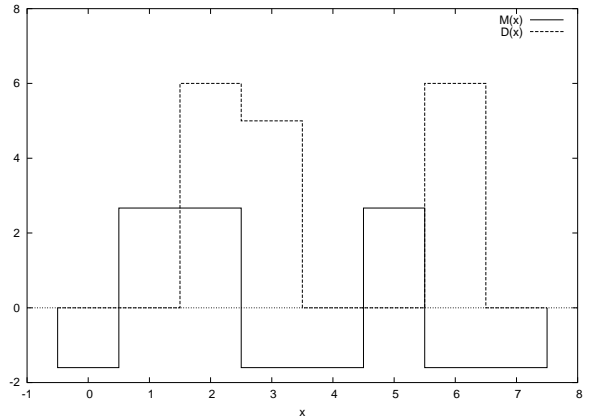


FIG. 3: $M(x)$ and $D(x)$ in 1-dimensional example

From the mathematical point of view the function $D(\vec{x})$ is the convolution of the mask function $M(\vec{x})$ with the source function $S(\vec{x})$ (see [HG], p. 18):

$$D(\vec{x}) = (M * S)(\vec{x}) \quad (4)$$

If we now choose $G(\vec{x}) \equiv M(-\vec{x})$, we get:

$$\begin{aligned} (G * M)(\vec{x}) &= \int G(\vec{z})M(\vec{x} - \vec{z})d\vec{z} \\ &= \int M(-\vec{z})M(\vec{x} - \vec{z})d\vec{z} \\ &= \int M(\vec{z})M(\vec{x} + \vec{z})d\vec{z} \\ &= \delta^{(2)}(\vec{x}) \end{aligned} \quad (5)$$

which is the autocorrelation function of $M(\vec{x})$. If $M(\vec{x})$ is a widely extended 2-dimensional array of independent random numbers, the autocorrelation function is almost a δ -function with a very sharp peak at $\vec{x} = 0$: $\delta^{(2)}(\vec{x})$.

With this approximation we get from equations (4), (5) and the associativity of the convolution:

$$\begin{aligned} (G * D)(\vec{x}) &= (G * (M * S))(\vec{x}) \\ &= ((G * M) * S)(\vec{x}) \\ &= \int \delta^{(2)}(-\vec{z})S(\vec{x} - \vec{z})d\vec{z} \\ &= S(\vec{x}) \end{aligned} \quad (7)$$

This means, that we can reconstruct the distribution of the sources by calculating the convolution of $G(\vec{x})$ with the detector data $D(\vec{x})$.

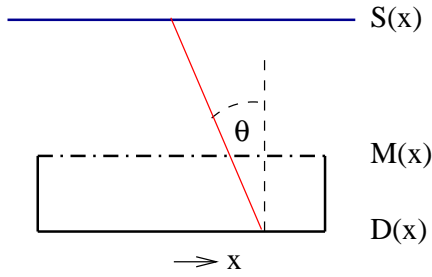


FIG. 4: 1-dimensional case: connection between $D(x)$, $M(x)$ and $S(x)$

If we use $M(-\vec{x})$ instead of $G(\vec{x})$, we arrive at:

$$\begin{aligned} S(\vec{x}) &= (G * D)(\vec{x}) \\ &= \int M(-\vec{z})D(\vec{x} - \vec{z})d\vec{z} \\ &= \int M(\vec{z})D(\vec{x} + \vec{z})d\vec{z} \end{aligned} \quad (8)$$

From this formula we can easily calculate the position of the sources.

III. PROGRAM

The intention of this project was

- on the one hand to write a computer program, which does the simulation of the measurement process, i.e. the counting of the photons coming from sources in specified directions with particular intensity, hitting a detector element, and
- on the other hand, to develop an analysis algorithm, which reconstructs the direction of the sources from the given detection rates of each detector pixel using the information about the layout of the mask.

In the following I give a description of the program "coded mask", the main element of this project.

The program is written in C and basically consists of 4 parts:

- **rndmask:** tool, which creates a coded mask using a random number generator
- **sample:** simulates the measurement process for one or several γ -ray sources
- **analyse:** uses the data output from "sample" to reconstruct the direction and intensity of the sources.
- **plot:** several tools to plot the mask, the detector data or a skyplot with the calculated positions and intensities of the sources

A. Mask creators

1. Random masks

The program "rndmask" creates a mask with a definite number of pixels in x- and y-direction and a desired opacity.

With these parameters the single Pixels and mask elements respectively are chosen transparent or opaque according to a random number generator, using the following format:

- "0" represents a mask element which is transparent for γ -rays
- "1" represents an opaque mask element

Figure 5 gives an example for a 64×64 -mask with an opacity of $2/3$ in



FIG. 5: randomly generated mask with 64×64 pixels and an opacity of $2/3$

Of course it might not be the best way to choose a mask in this simple way. But the result turns out to be quite good, even in comparison to masks actually used on satellites. So I have used the 64×64 random mask for testing.

2. MURAs

MURAs are an alternative to random masks with better reconstruction properties. They are created with prime numbers. You can find more about that in [HG], p. 28 f).

The mask of the MIRAX HXI telescope is a 151×151 MURA (see [M]). I have done some simulation with this mask, which you can see in figure 6.

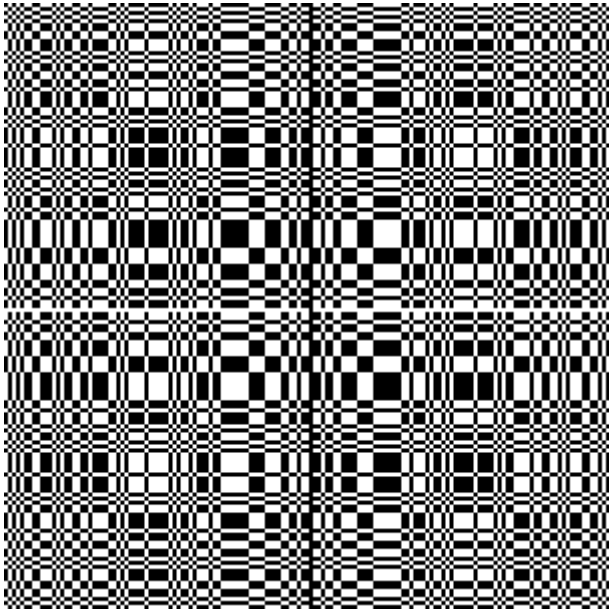


FIG. 6: 151×151 MURA of the MIRAX HXI imager

B. "sample"

The program "sample" simulates the measurement process in space, where γ -rays from different with particular intensity are hitting the detector through the mask. The results are the coordinate (i.e. the index) of the detector element, the time of the detection event and the energy of the single photon.

In principle "sample" consists of the three following files (and some additional header-files):

- **"sample.c"**: main part of the program
- **"read_mask_from_file.c"**: reads the mask layout from a file
- **"create_rnd_photon.c"**: creates a random photon according to a given source position
- **"intersection.c"**: calculates the intersection of a photon with the plane of the mask and the detector respectively

Important parameter files:

- **"../parameter.dat"**: main parameters like mask-file, detector-dimensions or output-file
- **mask-file**: layout of the mask (format see section III A 1)
- **"sources.dat"**: directions and intensities of the different γ -ray sources

Additional settings like the number of background photons are defined as constants within "sample.c".

At the beginning the program reads the settings, including the mask- and the source-file. The position of

each source is given as a direction in 3-dimensional space, using the polar angle θ and the azimuth angle ϕ of spherical coordinates. The intensity is specified as the number of photons per unit time passing a circle with reference area $A_{ref} = \frac{1}{4}d_{mask}^2\pi$, where d_{mask} is the length of the diagonal of the square mask.

The radius is chosen in such a way that the mask is entirely covered by the reference circle (see figure 7).

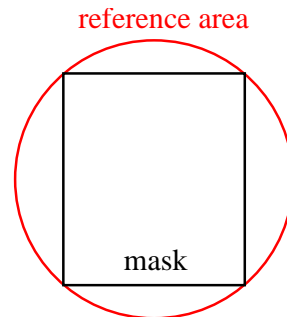


FIG. 7: reference area covering the mask

For the measurement process the simulation creates photons at a random position within the reference area. The reference circle can be imagined to lie perpendicular to the connection line between the mask and the source, as you can see in figure 8. 7.

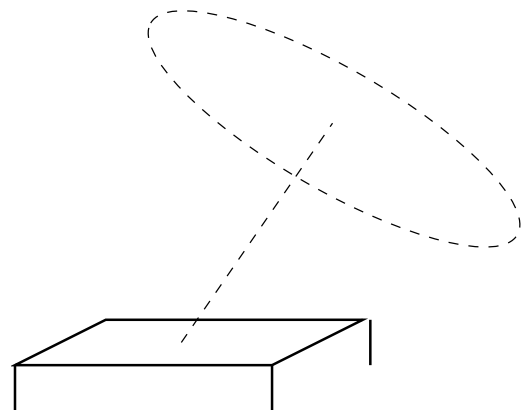


FIG. 8: reference circle according to the mask in 3-dimensional space

Of course the circle (or disk in 3-dimensional space) can be moved along the connection line without changing the intersection point of a photon with the plain of the mask. For convenience the center of the disk is chosen to be identical with the center of the square mask as the the origin of the coordinate system. From the side view this looks like in figure 9.

Figure 10 gives an example with 5000 photons randomly distributed on the reference disk in 3-dimensional space. With this coordinate system, in which the center of the disk and of the mask are identical, the intersection point of the line representing the flight of the randomly

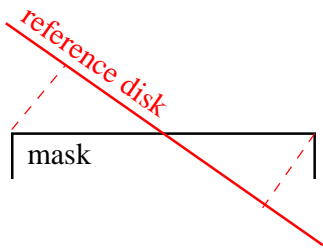


FIG. 9: sideview of the reference disk and the square mask with centers chosen to be identical

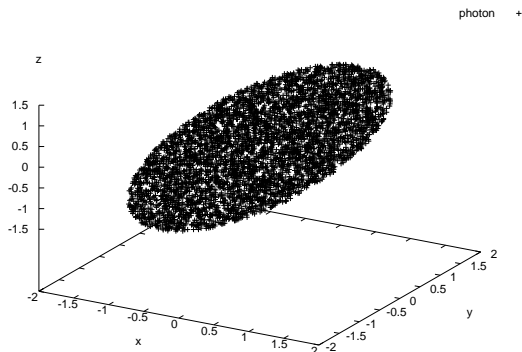


FIG. 10: randomly distributed photons of the reference circle

positioned photon with the the plain of the mask can be calculated easily.

If the photon misses the mask, it is lost in any case and will not be registered. Whereas, if it hits the mask, one has to decide, whether it passes through a transparent pixel or whether it is absorbed by an opaque mask element.

For $\theta = 0$ all photons passing the mask will hit the detector, but for $\theta \neq 0$ some of them are usually absorbed by the walls of the device. The intersection point of the transmitted photon with the detector plain is calculated with the same function as the intersection with the mask plain. Only the height of the plain in z-direction is different (the detector level is below the mask level).

If a transmitted photon hits the detector and not the walls, the coordinates of the affected detector element (integer numbers!) are written into the output file together with the time of the event and the energy of the photon, which is generally set to 1.0 for our purpose.

Apart from the photons coming from the γ -ray sources, there is a particular amount of photons registered by the detector, which is independent from outer parameters like source positions or the mask layout. These photons are randomly distributed over the entire detector area and simulate the background events in space, which are for example caused by imperfect screening.

Figure 11 displays the detector data for a source on the optical axis ($\theta = 0$) with some background radiation.

The brightness of each pixel represents the number of photons that have been registered by this pixel.

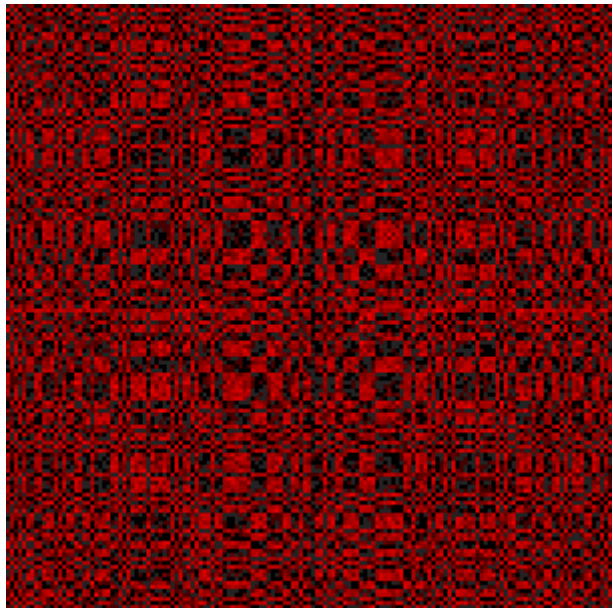


FIG. 11: plot of detector data $D(\vec{x})$ for a source on the optical axis

If you compare figure 11 with the mask in figure 6, you will certainly recognize the pattern of the mask in the detector data.

Figure 12 displays a plot for a slightly off-axis source with $\theta = 0.005$ and $\phi = \frac{\pi}{2}$.

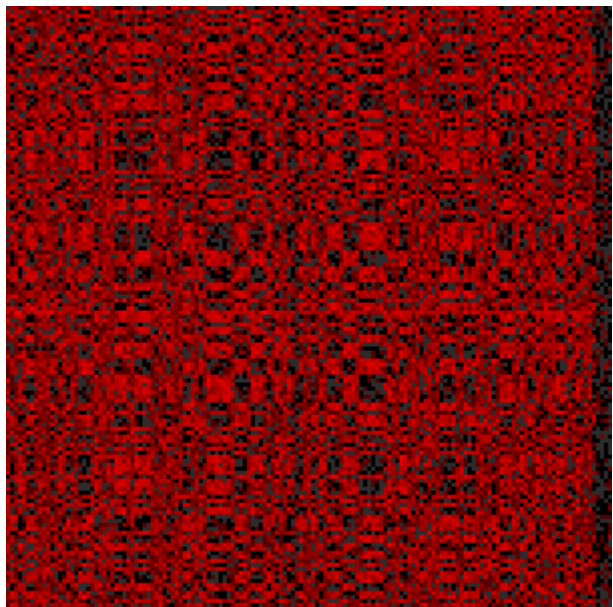


FIG. 12: plot of detector data $D(\vec{x})$ for an off-axis source at $\theta = 0.005$ and $\phi = \frac{\pi}{2}$

C. "analyse"

The program "analyse" processes the output data from "sample" and reconstructs the directions of the different sources with their intensities. It uses the same parameter file "../parameter.dat" as "sample" to ensure equivalent settings.

The main input data is on the one hand the mask file, and on the other hand the output file of "sample", which contains the coordinates of the detected photons. (The energy and detection time are neglected for our purpose.)

After all data is loaded from the files, the program calculates the convolution of the mask with the detector data according to equation 8 in section II E, i.e. the correlation function. You can clearly recognize the delta peak in figure 13 for an example with a source on the optical axis.

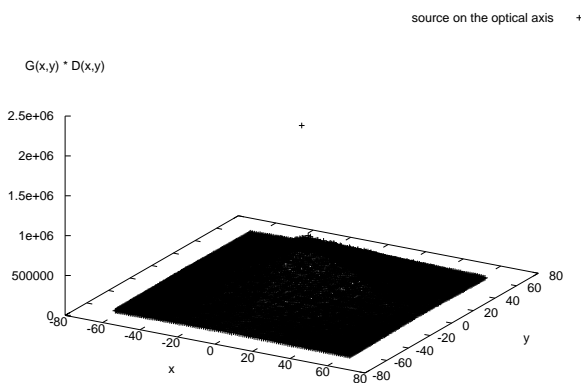


FIG. 13: delta peak of the correlation function for a source on the optical axis

Additionally the correlation is normalized according to the fact, that the power from the radiation on the detector depends on the polar angle θ (cf. section IV A). The bigger θ is, the lower is the power on the detector in comparison to the actual power of the source.

This effect is avoided by dividing the correlation by some reference term, which depends on deviation from $\vec{x} = 0$ (equivalent to $\theta = 0$) and takes into account the size of the actually available mask area and the cosine of the polar angle θ .

As there are only few mask pixels available, the denominator for the normalization becomes very small for \vec{x} -values close the edges, which might cause singularities. So the correlation for these \vec{x} -values is neglected (about 10 rows/columns from the edge).

The normalized convolution is written to the file "skyplot.dat", because it can be directly used to create a skyplot with the position and intensity of the different sources on the sky projection plane. A skyplot displays the positions of the sources on a projection plain from the point of view of the telescope (see figure 14).

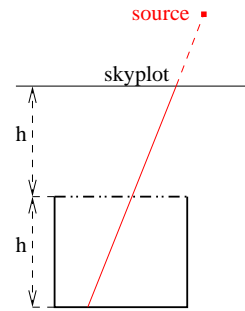


FIG. 14: principle of a skyplot

For additional analysis the program determines the position \vec{x}_{max} of the maximum of the normalized convolution. From \vec{x}_{max} , the width of one detector pixel, and from the height h of the device, i.e. the distance between mask and detector, the direction of the brightest source can be calculated easily in spherical coordinates.

The intensity of the source can also be determined from the height of the maximum peak in the convolution, whereas there might be some deviation from the actual value caused by background photons or the influence of other sources.

In order to find some sources with less intensity, the influence of the brightest source, which has already been determined, on the detector data is calculated and subtracted. Then the convolution is re-calculated again with the modified detector data in order to get the second brightest source, and so on.

For a single source the reconstruction of the source position from the mask pattern and the detector data might still be possible by simply looking at the detector plot, if you consider figure 14. But for several sources the shadow pattern is a superposition of shadows from several sources. In this case might not be so obvious at first sight, that it resembles the mask pattern.

As you will see in section IV B, the correlation is a powerful tool even to resolve several cells. (As long as they do not have too different intensities.)

The background radiation of photons, which are randomly distributed over the entire detector area in our model, is filtered out quite well by the correlation, as we would estimate from equation 2 in section II E (simulation data in section IV E).

Unfortunately calculation the correlation for a $N \times N$ -detector array with loops takes almost N^4 steps. So for large values of N it would be better to use an alternative method like fast fourier transformation according to the convolution theorem.

D. Plotting

There are three tools for plotting:

- **"plot_mask"**: displays the mask from "rndmask"

- **"plot_det_data"**: displays the detector data from "sample"
- **"skyplot"**: creates a skyplot from "skyplot.dat", which is an output of "analyse"

All of them create a ".png" file.

For these programs are neither really important for the actual simulation nor very complicated, I will not go into the here.

IV. SIMULATION DATA

In this chapter you will find the results of some particular experiments with the simulation, in order to make sure that it works properly.

A. Power as a function of θ

The radiation flux through the mask is determined by the position of the source (compare figure 15). It has a

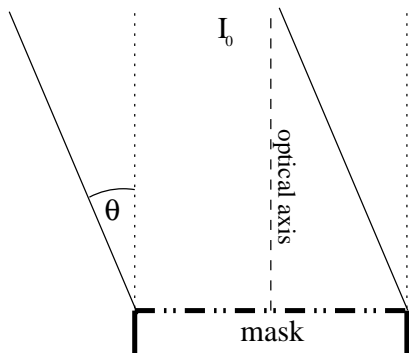


FIG. 15: radiation flux through the mask depends on the polar angle θ

maximum, if the source is on the optical axis (i.e. $\theta = 0$):

$$I_{mask} = I_0 \cdot \cos(\theta) \quad (9)$$

Since the detector is within a box of definite height, the walls of the box induce a shadow on the detector area (compare figure 16). If h is the height and b the width of the box, there is absolutely no radiation coming to the detector for $\theta_{max} \geq \arctan(\frac{b}{h})$, even if the mask is transparent everywhere. For $0 \leq \theta \leq \theta_{max}$ the radiation power on the detector can be calculated as

$$P(\theta) = P_0 \cdot \cos(\theta) \cdot (1 - \frac{h}{b} \cdot \tan(\theta)) \quad (10)$$

You can see the radiation power on the mask-area and on the detector-area (with the assumption of a totally

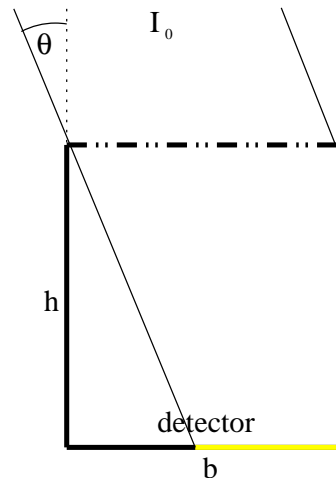


FIG. 16: radiation power on the detector area depends on the polar angle θ and the shape of the box

transparent mask) as a function of the polar angle θ ($\phi = 0$) for a box with height $h = 760$ and width $b = 130.6$ in figure 17. Obviously the simulation data matches the theoretical curves well.

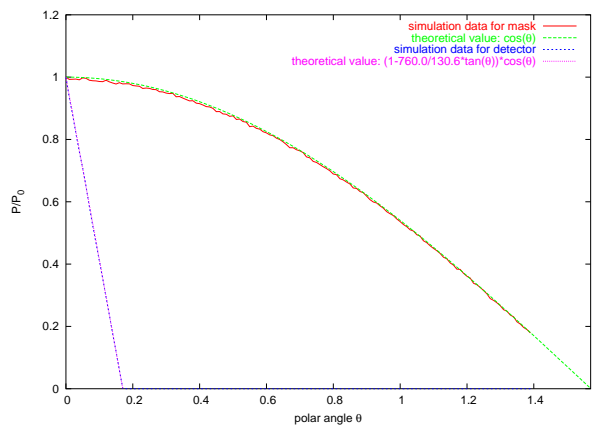


FIG. 17: radiation power on mask and detector as a function of the polar angle θ

This confirms, that the process of setting random photons on the reference disk and calculating their intersection with the mask and detector area in simulation code (program part "sample") is implemented correctly.

B. Skyplots

A skyplot is a graphical presentation of the convolution, calculated by "analyse". Bright points in the plot are caused by δ -peaks of the convolution and correspond to the source position on the sky projection plane.

For an example you can see a section of a skyplot with four sources in figure 18. The fact, that you only see three different points is caused by angular resolution effects

of the coded mask telescope. The upper point actually consists of two different sources, which lie very close to each other and have less intensity than the remaining two.

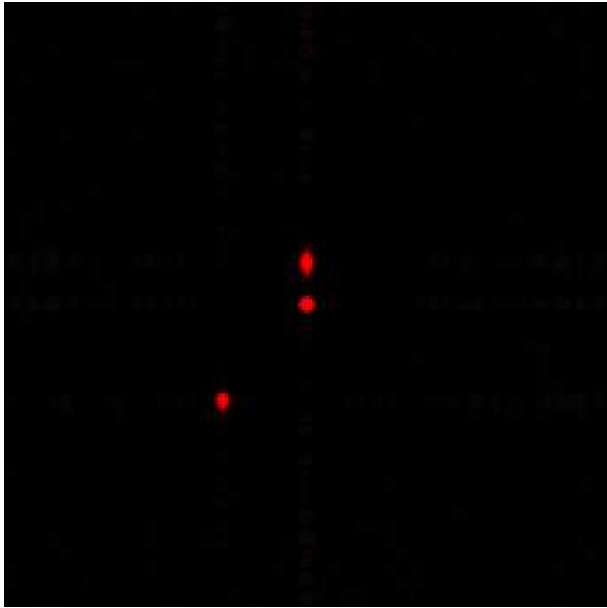


FIG. 18: section from a skyplot with four sources; the upper two of them are very close to each other and cannot be resolved

C. Angular resolution

The angular resolution of the coded mask telescope depends on the number and the width of its detector pixels. For they have finite size, we get the detector data from the measurement process only for discrete \vec{x} -values. So the program cannot resolve sources, which are too close together.

From the dimensions of the telescope, we can determine the minimum angular resolution for the polar angle:

$$\delta\theta = \arctan\left(\frac{d_{\text{pixel}}}{h}\right) \quad (11)$$

where $d_{\text{pixel}} = 865\mu\text{m}$ is the width of one detector pixel and $h = 76\text{cm}$ is the distance between the mask and the detector (cf. [M]).

With this data we get a theoretical angular resolution of $\delta\theta \approx 0.001138 \hat{=} 3.9'$, which is exactly the same as from the simulation: for a source at $\theta_{\text{in}} = 0.0005$ as an input for "sample", "analyse" returns a value of $\theta_{\text{out}} = 0.000000$, whereas for $\theta_{\text{in}} = 0.0006$ we get the next bigger value of $\theta_{\text{out}} = 0.001138$.

Of course, the angular resolution of the azimuth angle ϕ depends on the value of θ . The bigger θ the better is the resolution for ϕ .

If two sources are so close to each other, that they cannot be resolved, they are one wide spot on the skyplot, as you can see in figure 18 for the upper two sources.

D. Intensity

Additional to the angular resolution, the fact, that the detector consists of discrete pixels, has also an effect on the reconstruction of the source intensity. The detector cannot determine the exact position, where the photon hits the plain, but integrates over its single elements with a finite size.

If we assume e.g. $\phi = 0$ and choose θ in such a way, that one mask pixel is imaged on two detector pixels as in figure 19, the power coming through the transparent mask pixel is distributed among the two detector pixels.



FIG. 19: power of one mask pixel distributed among two detector pixels

Calculating the correlation, only the detector rate of one of both pixels is taken into account. So the reconstructed intensity value for the source is too low.

For $\phi \neq 0$ the radiation power can be even distributed among four detector pixels in general, so the deviation from the true value might be bigger (cf. figure 20).

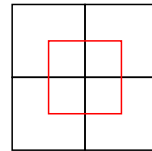


FIG. 20: power of one mask pixel distributed among four detector pixels

In figure 21 you can see the ratio of the calculated and the proper source intensity as a function of $\theta \in [0; 0.0016]$, i.e. for the shift over about one detector pixel in diagonal and 1. pixels in horizontal direction.

The minima with the biggest deviation lie between the maxima, where the calculated intensity is approximately the proper value, because of integer pixel shift.

The correct implementation of the normalization in section III C is proved by the fact, that **for integer shift** (i.e. each mask pixel is exactly imaged on one detector pixel) the calculated intensity is approximately equal to the proper value, over a wide range of $\theta \in [0; 0.158]$, as you can see in figure 22. ($\theta = 0.158$ is almost at the edge of the field of view.)

The deviation at large θ for the diagonal shift can be explained by the fact, that for this data the source is in

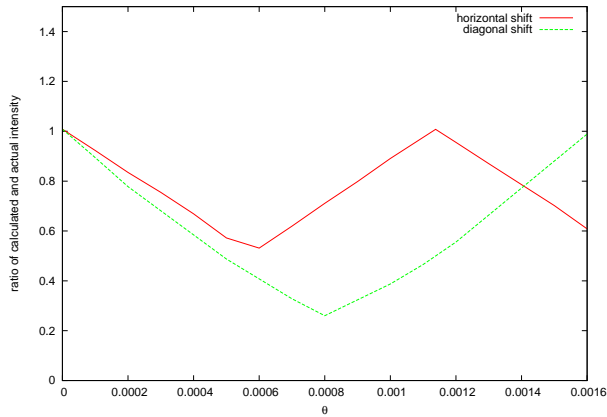


FIG. 21: calculated intensity deviates from the proper value due to discrete detector pixels

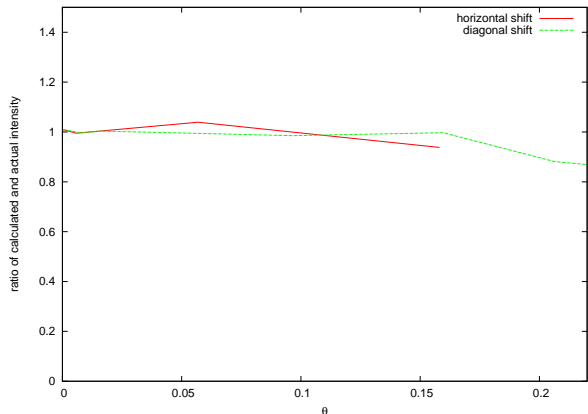


FIG. 22: ratio of calculated and actual source intensity is one over a wide range of θ . (In this plot only values of θ are taken into account, which correspond to integer shifts of the source on the sky projection plane. This proves that the intensity calculation would be correct, if we did not have a finite number of detector pixels.)

such a position, that only one corner of the detector can be reached by the radiation.

E. Weak sources

Additionally to the radiation from the sources in the field of view the detector also counts some background photons, because the environment cannot be perfectly screened off. If we observe a very weak source, the effect of the background radiation on the detector data might be so large, that the source cannot be located, because the peak in the convolution is too small in comparison to statistical fluctuations.

Of course we would like to know, whether our reconstruction code is good enough to determine real sources within a realistic environment.

From [M], p. 16 we can estimate a flux of background

photons of about $F_{bg} \approx 0.01 \text{s}^{-1} \text{cm}^{-2}$.

As an example of a real source we take the galactic center with a flux of $F_{gc} \approx 5.6 \text{mCrab}$ (see [NI], data of the IBIS instrument on the INTEGRAL satellite). ($1 \text{mCrab} = 1.36 \cdot 10^{-11} \text{erg s}^{-1} \text{cm}^{-2} = 1.36 \cdot 10^{-18} \text{J s}^{-1} \text{cm}^{-2}$)

The area of our detector is $A_{det} = (151.865 \cdot 10^{-6} \text{m})^2 \approx 170.6 \text{cm}^2$.

When the observation lasts for $\Delta t = 4 \text{h} = 14400 \text{s}$, the total number of background photons is about $N_{bg} \approx 25 \cdot 10^3$, i.e. on the average 1 photon on each of the 151^2 detector pixels.

If we assume a photon energy of about 30keV for the photons coming from the source, we get a number of $N_{gc} = \frac{5.6 \cdot 1.36 \cdot 10^{-18} \text{J}}{30 \text{keV}} \cdot 14400 \cdot 22 \cdot 10^3 \approx 0.52 \cdot 10^6$.

As the simulation "sample" distributes the source photons on the reference disk, we have to use a total number of $N_s = N_{gc} \cdot \frac{\pi}{2} \approx 0.79 \cdot 10^6$ source photons and N_{bg} background photons.

Using these parameters for the simulation, "analyse" calculated the position and the intensity of the source correctly. So the algorithm is good enough for real-environment simulations.

The correct data was even determined correctly for $N_{src} = 5000$ (at $\theta = 0.018$ and $\phi = \frac{\pi}{2}$), although there are too few photons to recognize the mask pattern in the plot of the detector data in figure 23. The source is hardly visible on the skyplot in figure 24.

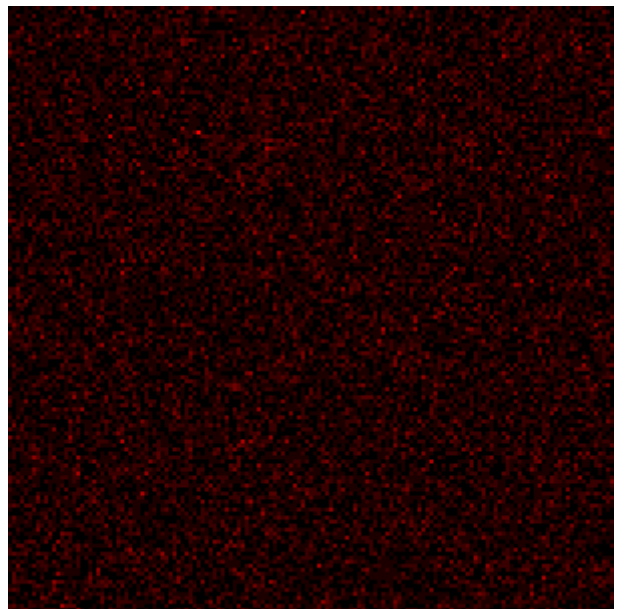


FIG. 23: detector data for a weak source at $\theta = 0.018$, $\phi = \frac{\pi}{2}$ with realistic background

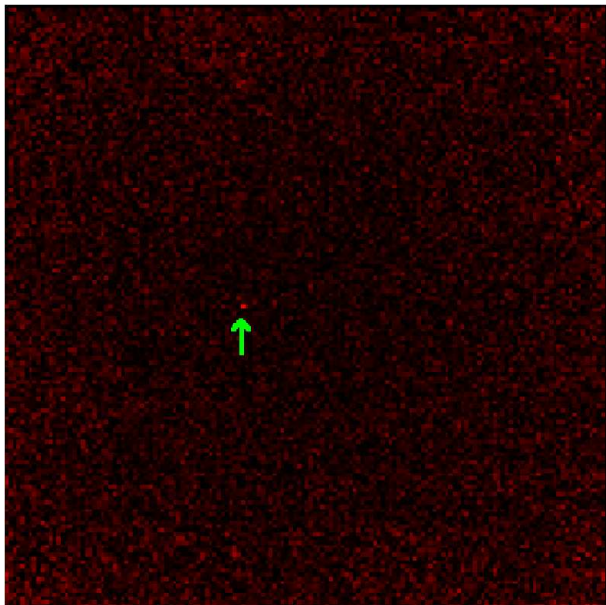


FIG. 24: skyplot for a weak source at $\theta = 0.018$, $\phi = \frac{\pi}{2}$ with realistic background

V. CONCLUSION

The simulation and the analysis code were written and tested with parameters similar to the MIRAX telescope,

although it is not a realistic model. It has some simplifications like a detector and mask of the same size with the same number of pixels and so on.

Apart from that it uses a realistic mask and has turned out to work quite well in a realistic environment with background radiation. It was especially surprising, that the mathematical methods of reconstructing the source position are operating even at very low source intensity.

Unfortunately there are some systematical errors on determining the original source intensity, because of the discrete detector pixels. I tried to avoid this problem by using virtual pixels, in order to get a smoother lattice. But the results from these simulations turn out to be exactly the same as for the original implementation.

With virtual pixels the fact that the processing time is proportional to N^4 turned out to be a big disadvantage of using loops for calculating the correlation function. This problem could be solved by using other methods like fast fourier transformation.

All in all the program can be seen a basis for developing advanced simulations on coded masks.

-
- [HG] Heiko A. Groeneveld: "Design, Simulation und Optimierung kodierter Aperturen", 1999, Tübingen
 [W] <http://de.wikipedia.org/wiki/Röntgenastronomie>
 [M] Richard E. Rothschild: "Hard X-ray Imaging for MIRAX", 2003, San Diego
 [UI] Ubertini et al.: "IBIS: The Imager on-board INTE-

- GRAL"
 [SH] <http://sebastian-hess.eu/roentgenphysik.html>
 [NI] <http://heasarc.nasa.gov/W3Browse/integral/intgcat.html>
 [FI] Fabian Frost: "INTEGRAL"